Title	Development of a wavelength-shifting-fibre-based scintillator neutron detector as an alternative to ^{3}He at J-PARC/MLF
Author(s)	Nakamura Tatsuya, To Kentaro, Honda Katsunori, Birumachi Atsushi, Ebine Masumi, Sakasai Kaoru, Soyama Kazuhiko, Katagiri Masaki
Citation	Journal of Physics; Conference Series, 528, p.012042_1-012042_7
Text Version	Published Journal Article
URL	https://jopss.jaea.go.jp/search/servlet/search?5041474
DOI	https://doi.org/10.1088/1742-6596/528/1/012042
Right	Content from this work may be used under the terms of the Creative Commons Attribution 3.0 licence. Any further distribution of this work must maintain attribution to the author(s) and the title of the work, journal citation and DOI. Published under licence by IOP Publishing Ltd

Development of a wavelength-shifting-fibre-based scintillator neutron detector as an alternative to ^{3}He at J-PARC/MLF

2014 J. Phys.: Conf. Ser. 528 012042

(http://iopscience.iop.org/1742-6596/528/1/012042)

Journal of Physics: Conference Series **528** (2014) 012042 doi:10.1088/1742-6596/528/1/012042

Development of a wavelength-shifting-fibre-based scintillator neutron detector as an alternative to ^{3}He at J-PARC/MLF

T Nakamura[1], K Toh[1], K Honda[1], A Birumachi[2], M Ebine[2], K Sakasai[1], K Soyama[1] and M Katagiri[3]

[1] J-PARC center, Japan Atomic Energy Agency, Tokai, Ibaraki 319-1195, Japan
[2] Nuclear Science Directorate, Japan Atomic Energy Agency, Tokai, Ibaraki 319-1195, Japan
[3] Frontier Research Center for Applied Atomic Sciences, Ibaraki University, Tokai, Ibaraki 319-1106, Japan

E-mail:nakamura.tatsuya@jaea.go.jp

Abstract. A wavelength-shifting-fibre-based scintillator detector has been developed as an alternative detector to ^{3}He gas. The detector is intended for use in an inelastic neutron-scattering instrument at J-PARC. The detector being developed, which is based on the one made for a SENJU diffractometer, is designed to cover a large scattering angle with a moderate pixel size as well as exhibiting a high detection efficiency, low gamma-ray sensitivity and low background count rate. A prototype detector with a pixel size of 20 × 20 mm and a neutron-sensitive area of 320 × 320 mm^2 has been constructed. This paper describes the design of the detector and its performance relative to the original SENJU detector.

1. Introduction

The recent worldwide shortage of ^{3}He gas has accelerated the development of neutron detector technologies that could be alternative to conventional ^{3}He-gas-based detectors [1, 2]. The neutron detectors used in a neutron-scattering experiment should exhibit position sensitivity, high detection efficiency, low gamma-ray sensitivity and the capability of detecting high count rates. A particular requirement of detectors for use in an inelastic neutron-scattering (INS) instrument is that they should cover a large solid angle around a sample, with a typical requirement of several tens of square metres.

Several gas-based and scintillator-based neutron detectors are commercially available, such as those using a BF_3 gas, a thin film of ^{10}B or ^{6}Li, or a ZnS/^{6}LiF scintillator, but none of them satisfies the detector specifications required for an INS instrument. Current international research and development collaborations are investigating the use of such instruments in neutron-scattering experiments [3]. These projects can be categorized into three lines of development: a gas-based detector with a ^{10}B converter film [4], a BF_3 gas-based detector [5] and a scintillator-based detector [6].

This paper presents the development status of our detector incorporating a scintillator based on wavelength shifting (WLS) fibre, as well as the design and detection performance of a prototype detector.

2. Detector design for an INS instrument

Our detector employs detector technologies developed for the SENJU instrument [7]. SENJU is a single-crystal Laue instrument constructed in the Materials and Life Science Experimental Facility at the Japan Proton Accelerator Research Complex (J-PARC/MLF) [8]. Table 1 summarizes the typical detector specifications for a position-sensitive ^{3}He-gas tube used in an INS instrument and the original SENJU scintillator detector installed at J-PARC/MLF. To make a detector that would be a suitable alternative to a ^{3}He-gas detector, the SENJU detector should be redesigned to fulfil the requirements for detection efficiency, background count, pixel size and detector spatial coverage, together with a low manufacturing cost. Moreover, the anticipated detector for an INS instrument should be modular in design and cover an area of several tens of square metres.

Figure 1 is a diagram of a large-area detector unit for an INS instrument. The detector unit covers a total neutron-sensitive area of 1.64 m^2 with a packing density of 79%, with each detector unit comprising 16 detector modules. One detector module has a neutron-detecting area of 320 × 320 mm^2 with a pixel size of 20 × 20 mm^2.

Table 1. Specifications for a ^{3}He-gas tube and the SENJU detector. The latter is a position-sensitive scintillator detector used in the SENJU diffractometer at J-PARC/MLF.

Detector characteristics	^{3}He detector*	SENJU *detector*
Neutron efficiency	70% at 1 Å	20% at 1 Å
Gamma sensitivity	10^{-6}	10^{-6}
Background	~10^{-5} 1/cm^2/s	2×10^{-4} 1/cm^2/s
Spatial resolution (*X*)	25 mm	4 mm
Spatial resolution (*Y*)	15 ~ 25 mm	4 mm
Local rate capability	50 kHz on a pixel	<50 kHz
Global rate capability	50 kHz on a tube	<50 kHz
Time resolution	1 μs	2 μs
Area/det	0.025 m^2	0.065 m^2
Environment	Cryogenic vacuum	In air

* ^{3}He 10 bar, 25-mm diameter, 1 m long

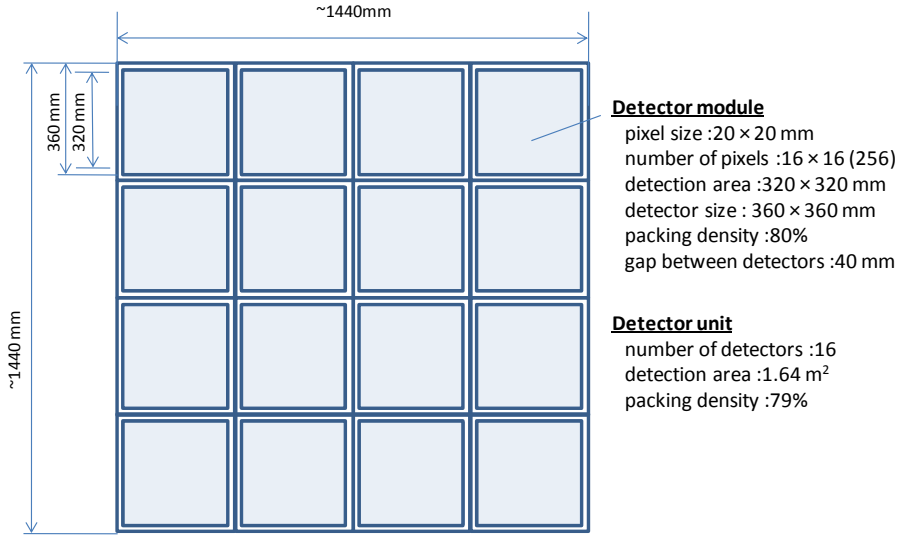

Figure 1. The design of a detector unit for an INS instrument.

3. Development of a large-area scintillator detector module

3.1. Increasing the pixel size and detection area

Figure 2 shows a schematic view of the neutron-detecting head of the scintillator/WLS-fibre-based detector module. A pitch of the WLS fibres is 5 mm, in contrast to 4 mm in the original SENJU detector, which increases the neutron-sensitive area of the detector by a factor of 1.56. The pixel size can be made larger (i.e. 20 × 20 mm^2) by reading out four WLS fibres as one channel while maintaining a reasonable light-collection efficiency. Technically these four WLS fibres are coupled to one pixel by of a multianode photomultiplier tube (MA-PMT).

The light-collection efficiency of the WLS-fibre-based detector was evaluated by measuring the photoelectron (PE) number distribution (PND) detected with mock-up detectors. Detectors constructed with WLS fibres at pitches of 4 mm and 5 mm were prepared for this test. A scintillator and MA-PMTs with the same parameters were used to facilitate the comparison of PNDs.

Figure 3 shows the PNDs measured with the detectors. A ZnS/$^{10}B_2O_3$ scintillator screen was implemented in the detectors [9, 10]. To reject false triggering events that occurred due to afterglow, the PNDs were measured only when more than three PEs were detected in both the x and y WLS fibre arrays within a 2-μs gated window. This operating condition was also used in the original detector [7]. The measured PNDs had modes at 13 PEs and 12 PEs for the detectors with pitches of 4 mm and 5 mm, respectively. These modes varied with the threshold setting of each WLS fibre array, but the PNDs actually represented distributions of the detected number of PEs that were accepted by the signal processing and encoder electronics.

The mean number of detected PEs was calculated as

$$(\text{mean number of PEs}) = (\Sigma C_i\, i)/(\Sigma C_i)$$

where i is the number of detected PEs and C_i is the count at an i. The corresponding mean numbers of detected PEs were 23.3 and 21.5, respectively. The mean light-collection efficiency decreased by only ~8% when the pitch of WLS fibres in the detector increased from 4 mm to 5 mm.

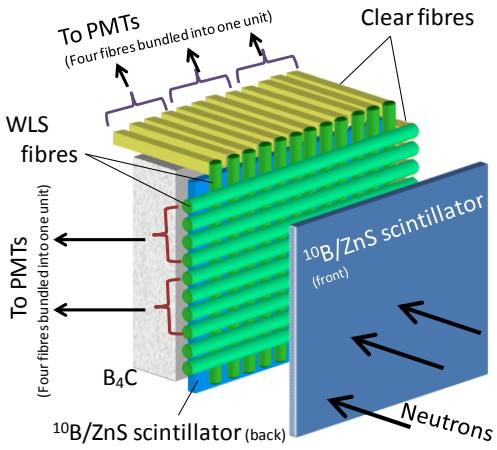

Figure 2. Schematic view of the neutron-detecting head of the scintillator/WLS-fibre-based detector.

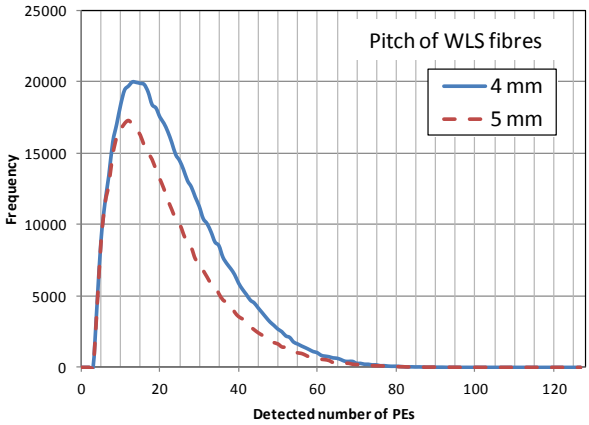

Figure 3. Distribution of the detected number of PEs measured with the WLS-fibre-based detector that was implemented with a ZnS/$^{10}B_2O_3$ scintillator screen.

3.2. PMTs for the detector

The prototype detector should be equipped with a PMT that has sufficient gain and uniformity, and a low background count. An MA-PMT can fulfil these requirements and is particularly effective in reducing the manufacturing cost of a detector. Four candidate MA-PMTs for a prototype detector were selected, and their adaptabilities were evaluated. Table 2 summarizes the specifications of the selected MA-PMTs. These MA-PMTs were chosen because their photocathode area is capable of accommodating four 1-mm-diameter fibres (corresponding to an area exceeding 4 mm^2). The R12445 and R11265-100 PMTs, which have been released on the market, have a larger pixel size than the conventional H8711-300 and H8804 MA-PMTs, which would ease the requirement to combine four fibres into one pixel. Their photocathode size of 6 × 6 mm would also be effective in reducing signal crosstalk between neighbouring pixels.

Table 2. Specifications of the evaluated multianode PMTs.

PMT type	No. of pixels	Pixel size	Max rating voltage
H8711-300	16	4 x 4 mm	-1000 V
H8804	64	2 x 2 mm	-1000 V
R12445	16	6 x 6 mm	-1100 V
R11265-100	64	3 x 3 mm	-1100 V

Figure 4a and b show the uniformity of the scanned PMT gains over the photocathode and the mean PMT gain as a function of the PMT voltage, respectively. The gain uniformity was measured by illuminating the photocathode area via a 0.2-mm-diameter optical fibre by a blue LED placed close to (~0.5 mm) the end of the fibre. The PMT gains at the centre of the pixel varied over the range 0.8–1.2 for all of the tested PMTs. This range of variations was acceptable for our detector. The mean PMT gain was much lower for the R12445 and R11265-100 PMTs than for the other devices (Figure 4b), which made them unsuitable for a prototype detector since a gain of at least 5×10^6 is required at the first stage of our photon counting electronics. Among the tested MA-PMTs, the H8711-300 device exhibited the best gain uniformity and overall gain. Its gain reached 5.5×10^6 when using a reasonable applied voltage of –900 V (corresponding to 90% of its maximum rating). This PMT has an ultra-bialkali photocathode, which is suitable for detecting shifted green light that has propagated through a WLS fibre, and hence the H8711-300 was used to construct a prototype detector.

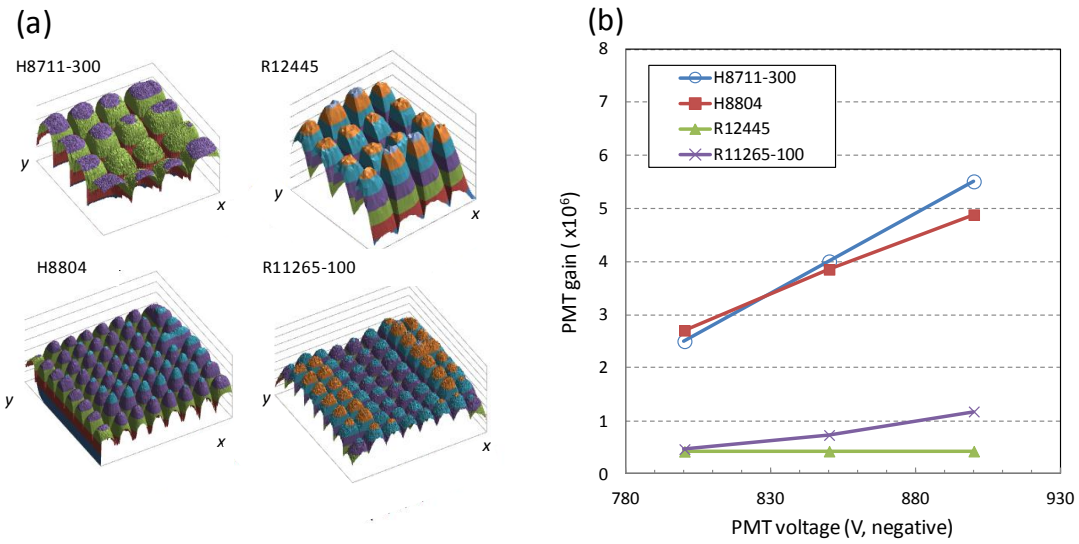

Figure 4. (a) Pixel-by-pixel PMT gain uniformity and (b) mean PMT gain versus the applied PMT voltage.

3.3. Detector electronics cards for a prototype detector

New detector electronics cards were produced for a prototype detector: (a) comparator cards, (b) a signal processing and encoder card and (c) a high-voltage card for driving the PMTs. All of these cards were designed to conform to the VME-3U size standard. Each of these cards was implemented in the prototype detector.

The comparator board that handles 32 analogue inputs and is equipped with a fast comparator chip (ADCMP605, Analog Devices) ensures a delay time of only ~1.6 ns. The card dissipates 7.4 W with a power supply of ±5V (corresponding to ~230 mW/channel).

The signal processing and encoder card accepts 2 of 32 digital signals. Field-programmable gate arrays (Cyclone II, ALTERA) operates at a clock frequency of 100 MHz. The functions of the board are similar to those in the original detector [7]: photon counting on each input channel, *x*-*y* coincidence, position calculation and data transfer to/from data-acquisition electronics. An optical-fibre link is implemented for data transmission, which makes the system robust in an electrically noisy environment.

The high-voltage card provides two outputs to bias the PMTs. Each output can supply a voltage up to –1250 V (at a maximum of 0.5 mA). The use of a dedicated high-voltage card decreases the cost of a medium-size detector system that requires less than 100 high-voltage channels compared to the commercial system. The card can be operated in either local or remote mode. The local mode enables a detector to operate in a stand-alone manner, where the setting of the PMT voltage is recorded in the on-board memory.

4. Detection performance of the prototype detector

The detection performance of the prototype detector was evaluated in terms of its detection efficiency, gamma-ray sensitivity and background count rate. The prototype detector was irradiated with neutrons from a ^{232}Cf source with a radioactivity of 1.83×10^{7} Bq that was set in the centre of a graphite moderator block of size 800 × 800 × 800 mm^3. The detector was placed 900 mm from the source. The gamma-ray sensitivity was measured using a ^{60}Co source with a radioactivity of 8.3×10^{5} Bq. The ^{60}Co source was positioned 200 mm from the scintillator, where the incident fluence was estimated to be $\sim1.7\times10^{5}$/s/detector. The gamma-ray sensitivity is defined as the probability of counting a gamma ray for a single incident photon. The background count rate was measured with no specific shielding implemented for the environmental radiation.

Figure 5a and b show photographs of the front and rear views of the prototype detector, respectively.

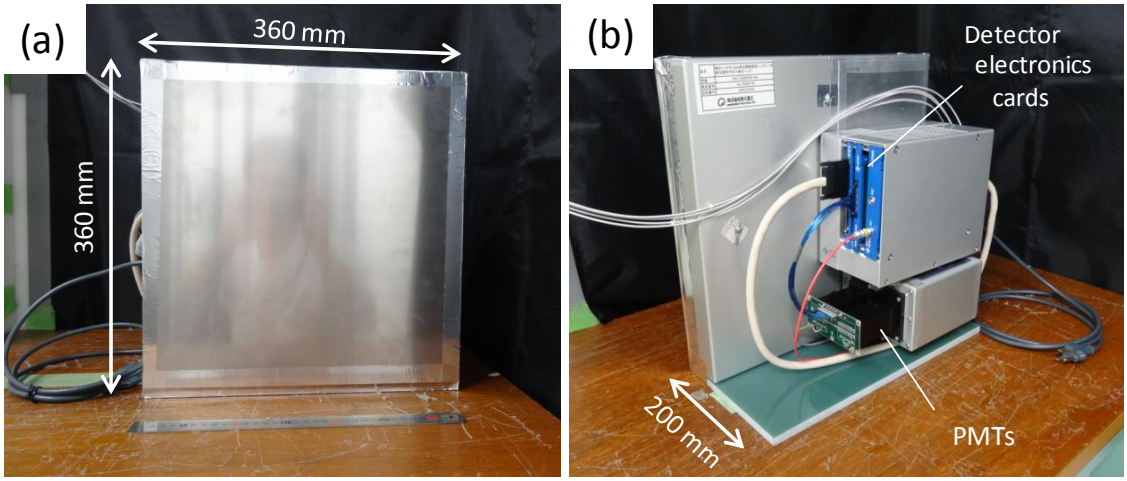

Figure 5. Photographs showing (a) front and (b) rear views of the prototype detector.

The detector was designed to be compact and light, with a physical size of 360 × 360 × 200 mm^3 and a weight of 11.6 kg. All of the detector electronics—including PMTs, the amplifier/discriminator card, the high-voltage card and the signal processing/encoder card—were installed behind the case housing the neutron-detecting head. The detector can be powered using either ±5 V DC or 100 V AC. The data were transferred using four optical fibres, with a maximum data transfer rate of 160 kcps at present. This transfer rate could be improved to more than 500 kcps by replacing the LED driver with a device with a faster time response.

Figure 6 shows the detector metrics, with the neutron count (detection efficiency) plotted versus the ^{60}Co gamma-ray sensitivity. The data measured with the original detector are included for comparison. At the ^{60}Co gamma-ray sensitivity of 10^{-6} (the normal operating condition), the prototype detector exhibited larger neutron counts than the original detector, with a calibrated detection efficiency of about 40%. The PND was evaluated with the prototype detector using a method similar to that described in Section 3.1. The mode and mean numbers of detected PEs were 16 and 27.6, respectively. These values are about 30% larger than those measured with the original detector, and indicate the better detection efficiency of the prototype detector, which could be due to its higher operating PMT gain.

Figure 7 shows the background count rate plotted versus the ^{60}Co gamma-ray sensitivity. In both detectors the background count rate decreased as the gamma-ray sensitivity decreased. For a ^{60}Co gamma-ray sensitivity of 10^{-6}, the background count rates were 2×10^{-4} cps/cm^2 and 4×10^{-4} cps/cm^2 for the original and prototype detectors, respectively. Although these values are typical of our WLS-fibre-based scintillator detectors, they were about an order larger than that of the conventional position-sensitive ^{3}He detector (~1×10^{-5} cps/cm^2). Possible sources of the background count are cosmic rays and contamination of the radioactive elements in the detector components. This should be clarified in future experiments.

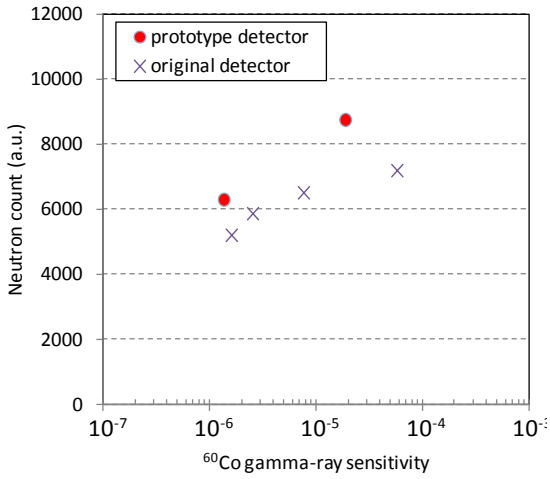

Figure 6. Neutron count versus ^{60}Co gamma-ray sensitivity.

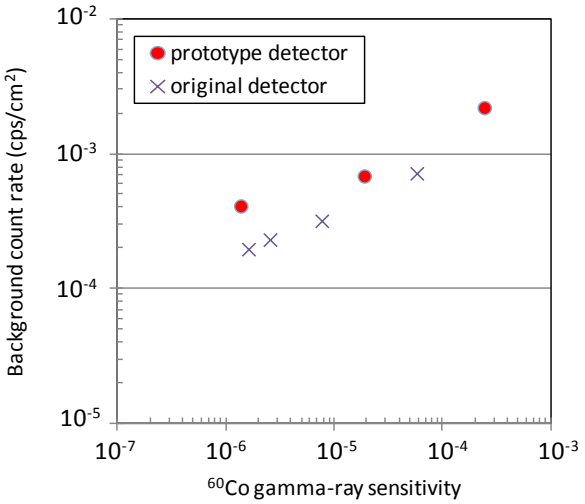

Figure 7. Background count rate versus ^{60}Co gamma-ray sensitivity.

Figure 8a and b show a flood image measured with a ^{232}Cf source and count frequencies in the *x* and *y* projections, respectively. An entire detector area was irradiated with thermal neutrons; in this experiment scintillator screens with dimensions of 256 × 256 mm^2 were implemented in the detector. The count uniformity was evaluated as 15.1±1.5% (mean±SD) by Gaussian fitting, which would be acceptable for most neutron-scattering experiments.

Finally, the specifications and detection performance of the prototype detector are summarized in Table 3.

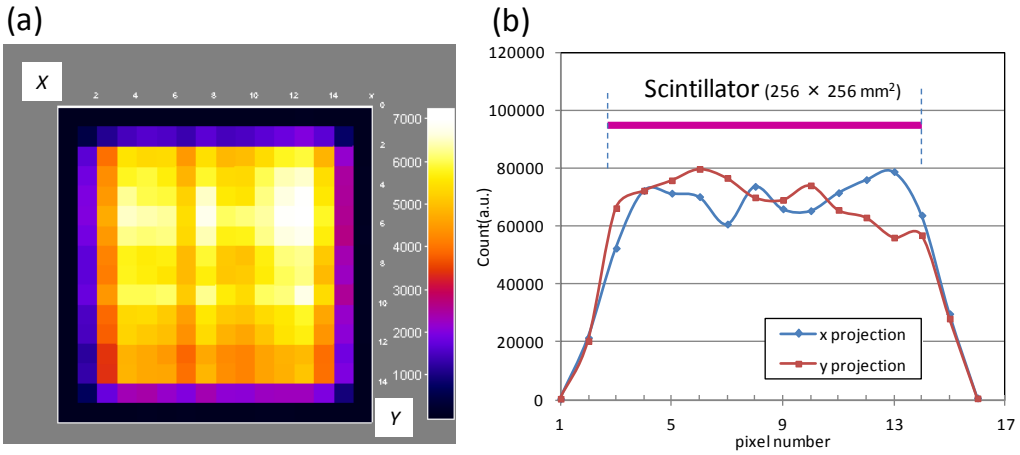

Figure 8. (a) Flood image and (b) count frequency in *x* and *y* projections measured with the prototype detector.

Table 3. Specifications and detection performance of the prototype detector.

Neutron-sensitive area	:	320 × 320 mm^2 (256 × 256 mm^2 at present)
Pixel size	:	20 × 20 mm^2
Detector efficiency	:	40% for 1.8 A
Gamma sensitivity	:	1×10^6
Background count	:	4×10^{-4} cps/cm^2
Count uniformity	:	15 ± 2%
Physical size	:	360 × 360 × 200 mm^3
Weight	:	11.6 kg
Power dissipation	:	13 W

5. Summary

A prototype scintillator/wavelength-shifting-fibre-based detector has been developed for an INS instrument as an alternative to a ^{3}He-gas detector. The detector parameters are designed specifically for an INS instrument, with a pixel size of 20 × 20 mm^2 and a neutron-sensitive area of 320 × 320 mm^2. The detector exhibited a detection efficiency of 40% for thermal neutrons and a gamma-ray sensitivity of 10^{-6}. Further work will include reducing the intrinsic background signal of the detector to the level of conventional position-sensitive ^{3}He detectors.

References

[1] United States Government Accountability Office 2011 *Managing critical isotope* GAO-11-472
[2] Kouzes R T 2009 *The ^{3}He supply problem* Report PNNL-18741 Pacific Northwest National Laboratory
[3] Zeitelhack K 2012 *Neutron News* vol. **23** No 4 10
[4] Bigault Y, et al 2012 *Neutron News* vol. **23** No 4 20
[5] Wilpert T 2012 *Neutron News*, vol. **23** No 4 14
[6] Rhodes N J 2012 *Neutron News*, vol. **23** No 4 26
[7] Nakamura T, et al. 2012 *Nucl. Instr. & Meth*. A **686** 64
[8] Tamura I., et al. 2012 *Journal of Physics: Conference Series* **340** 012040
[9] Kojima T, Katagiri M, Tsutsui N, Imai K, Matsubayashi M and Sakasai K, 2004 *Nucl. Instr. & Meth*. A **529** 325
[10] Nakamura T, et al. *Development of a ZnS/$^{10}B_2O3$ scintillator with low-afterglow phosphor Journal of Physics: Conference Series* in these proceedings